LA MÉTROLOGIE AU CŒUR DES TECHNOLOGIES CONTEMPORAINES

Metasurface for direction of arrival estimation
Métasurface pour l'estimation de la direction d'arrivée

N. Meftah[1], B. Ratni[1], M. N. El Korso[2], S. N. Burokur[1]

[1] LEME, Univ Paris Nanterre, F92410 Ville d'Avray, France, sburokur@parisnanterre.fr
[2] Université Paris-Saclay, CNRS, CentraleSupélec, Laboratoire des signaux et systèmes, 91190 Gif-sur-Yvette, France

Keywords: metasurface, reconfigurability, direction of arrival.
Mots clés : métasurface, reconfigurabilité, direction d'arrivée.

Abstract/ Résumé

A metasurface solution for the estimation of direction of arrival of electromagnetic waves is presented. The metasurface, which is programmable, is used as a reflector with an adjustable pointing direction to scan the azimuth plane for sensing and reflecting incoming waves to a power detector placed at a focal point, thereby estimating the incident direction. Furthermore, in order to achieve rapid and precise direction of arrival (DOA) estimation, a processing layer based on a pre-trained multilayer neural network is exploited to interpret variation in recorded power levels.

Une solution à base de métasurface est présentée pour estimer la direction d'arrivée des ondes électromagnétiques. La métasurface, qui est programmable, est utilisée comme un réflecteur où la direction de pointage est ajustable pour scanner l'azimut afin de capter et réfléchir les ondes incidentes vers un détecteur de puissance placé à un point focal, et ainsi estimer la direction d'arrivée. De plus, afin d'obtenir une estimation rapide et précise de la direction d'arrivée (DOA), une couche de traitement basée sur un réseau neuronal multicouche pré-entraîné est exploitée pour interpréter la variation des niveaux de puissance enregistrés.

1 Introduction

Direction of arrival (DOA) estimation, which consists in finding the direction of incoming waves, holds a major role in communications [1], localization [2] and tracking [3]. Due to its importance, various calculation methods and hardware structures have been developed in this field. In a general manner, DOA is estimated through the use of phased array antennas and various calculation methods [4], ranging from beamforming with Fast Fourier Transform (FFT) technique to algorithms such as MUSIC and ESPRIT [5]. Despite their remarkable resolution and accuracy, these algorithms present limitations in terms of computational and storage resources and their performance is significantly degraded for non-ideal conditions and imperfect antenna arrays.

Metasurfaces, which are composed of subwavelength unit cells, present the ability to manipulate electromagnetic waves at a subwavelength scale [6]-[8]. Hence, metasurfaces enable to design specific phase distributions that allow to manipulate scattering patterns [9]. As such, a programmable metasurface combined to a single receiver enables to to extract direction information from variations in received power levels [10]-[12]. Deep learning algorithms have recently been proposed as interesting methods to treat complex problems while requiring moderate computational resources [13]-[14]. Hence, artificial intelligence appears to be a complementary method with respect to traditional algorithms for direction finding from simple and low-cost systems. A metasurface, assisted by artificial intelligence, has also been applied for efficient and accurate DOA estimation [15]. However, large amounts of data are still required, and computations remain time-consuming.

Here, we present a programmable flat metasurface reflector where the pointing direction can be adjusted by varying its voltage-controlled phase profile to scan the azimuth plane for DOA estimation. By continuously varying the pointing direction of the metasurface reflector, a series of power levels received by the detector is measured and recorded. When the received power level reaches a maximum, the corresponding pointing angle enables estimating the DOA. Then, a processing layer based on a pre-trained multilayer neural network is exploited to interpret the subtle variations in recorded power levels, enabling both fast and accurate DOA estimation without refining the scanning step of the metasurface reflector. Hence, the proposed system is able to estimate the DOA with an accuracy of 1° for a coarse angular scanning of the azimuth plane with step of 5°.

2 Platform architecture for DOA estimation

The schematic of the platform architecture exploited in this study to estimate the DOA is illustrated in Fig. 1. A programmable metasurface operating around 10 GHz, as designed in [16]. The metasurface is composed of 30 × 30 unit cells with periodicity p = 6 mm. Each cell consists of two copper strips having a width w = 0.5 mm and separated by a gap g = 1.9 mm incorporating a voltage-controlled varactor diode, all printed on a 1.52 mm thick dielectric substrate with relative permittivity ε_r = 4.5. The metasurface is used as an electronically scannable reflector to redirect incoming signals toward a radiofrequency power detector at a focal point to record the power level for each electronic scanning. The phase profiles are electronically adjusted by a voltage control system biasing the varactor diodes incorporated in the metasurface. Cylindro-parabolic phase profiles are applied to the metasurface as

$$\phi(x) = \frac{2\pi}{\lambda}\left(\frac{(x-x_0)^2}{4F}\right) + \phi_0 \qquad (1)$$

where λ is the free space operating wavelength, F (= 30 mm) is the focal distance, and ϕ_0 denotes the reflection phase at location x_0. The orientation of the virtual parabola is controlled by shifting x_0 from its original position for a specific reception direction in the azimuth plane.

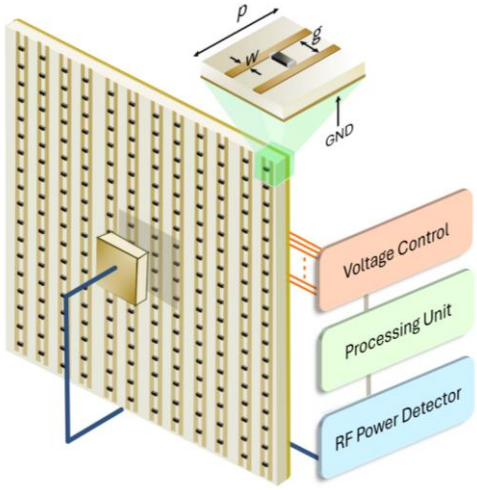

Figure 1: Architecture of the direction of arrival estimation system based on a programmable metasurface used as a parabolic reflector and a receiving antenna positioned at the focal distance. The geometric dimensions of the unit cell composing the metasurface are: p = 6 mm, w = 0.5 mm and g = 1.9 mm.

The first step consists in having a library of phase profiles versus pointing directions of the metasurface reflector. Hence, a patch antenna is placed at the focal point to illuminate the metasurface reflector, and the two are mounted and fixed on a rotating plate. A receiving horn antenna is fixed at a distance of 3 m to measure the wave reflected by the metasurface when the plate is rotated from -90° to +90°. The two antennas (patch and horn) are both connected to a network analyzer and far-field measurements are performed for different parabolic phase profiles corresponding to specific x_0 offsets. 17 phase profiles, corresponding to 17 pointing angles from -40° to +40° by step of 5°, are selected to establish the library (Table I).

x_0 (mm)	-38	-34	-28	-24	-18	-14	-10	-6	0	+6	+10	+14	+18	+24	+28	+34	+38
θ (°)	-40	-35	-30	-25	-20	-15	-10	-5	0	5	10	15	20	25	30	35	40

Table 1: Cylindro-parabolic phase profiles applied for DOA estimation: corresponding scanning angles for x_0 shifts.

3 Deep learning algorithm and model training

For the DOA estimation, the patch antenna is connected to a spectrum analyzer, which acts as a radiofrequency (RF) power detector. A horn antenna is used at the transmitter end in the far-field region and is positioned on a semi-circular rail to launch electromagnetic waves within an azimuth angular range of -40° to +40° with a step as fine as 1° (81 different directions of arrival) toward the metasurface at the receiving end, as presented in Fig. 2a.

The 17 cylindro-parabolic phase distributions are sequentially applied to the metasurface reflector at the receiver end to scan the azimuth plane from -40° to +40° with 5° step. Hence, for each tested angle of arrival, the acquisition system records 17 power levels. The power levels collected at the end of the angular scanning process are then utilized during the estimation phase by a pre-trained Multilayer Perceptron (MLP) model to accurately estimate the DOA with a step resolution of 1°.

The 17 power levels correspond to the features of a sample associated with a given arrival angle. This procedure is repeated two more times for each arrival angle, resulting in a dataset of 243 samples distributed over 81 different targets. It should be noted that training models require a large amount of data to ensure proper generalization and prevent overfitting. To increase the size of our dataset without requiring additional experimentally measured data, a data augmentation technique is used to generate additional data instances. As such, Gaussian noise mimicking natural variations and experimental disturbances observed on the original samples, is introduced. Hence, for each sample in the initial dataset, five new samples are generated to achieve an augmented dataset of 1215 samples. This augmentation approach ensures the integrity of the data by avoiding to introduce bias or transformations that could alter the physical nature of the original data.

Before training, the data is subjected to a structured preprocessing pipeline comprising three steps to standardize the features and maximize the model's performance [17]. First, data normalization is performed by dividing each instance by its maximum, corresponding to bringing the measured floor to zero. Second, a logarithmic transformation is performed to amplify subtle variations in power levels, improving the distinction between features associated with closely spaced incoming angles and enhancing prediction accuracy. Finally, the data is standardized to have a zero mean and unity variance to ensure comparable training conditions across models. For each of the 17 features, the mean and the standard deviation over all samples related to the j^{th} feature are calculated and then applied in the following transformation:

$$x_{ij}^{std} = \frac{x_{ij}^{norm} - \mu_j}{\sigma_j} \qquad (2)$$

where x_{ij} is the value of the feature j for the sample i, and *norm* denotes the normalized data. The dataset is then decomposed into training and test sets, with 80% of the data intended for training and 20% reserved for efficiently testing the performance of the trained model on unseen data.

The MLP training model composed of several fully connected layers of neurons is considered. For evaluating the performances, we use the mean square error (MSE), which is given by:

$$MSE(\boldsymbol{y}, \hat{\boldsymbol{y}}) = \frac{1}{n}\sum_{i=1}^{n}(y_i - \hat{y}_i)^2 \qquad (3)$$

where $\boldsymbol{y} = [y_1, \dots, y_n]$ and $\hat{\boldsymbol{y}} = [\hat{y}_1, \dots, \hat{y}_n]$, in which y_i is the real DOA value for the i^{th} sample and $\hat{y}_i$ is the value predicted by the model. The MSE is minimized by the iterative learning of weights w and biases b, which is done by backpropagation and gradient descent. Adjustments are therefore made as:

$$w_{mn}^{(l)} = w_{mn}^{(l)} - \alpha \frac{\partial \text{MSE}}{\partial w_{mn}^{(l)}} \qquad (4)$$

$$b_{m}^{(l)} = b_{m}^{(l)} - \alpha \frac{\partial \text{MSE}}{\partial b_{m}^{(l)}} \qquad (5)$$

where α is the learning rate, controlling the size of the steps made in the opposite direction of the gradient to reach a local minimum. $w_{mn}^{(l)}$ is the weight between the n^{th} neuron in the $(l\text{-}1)^{\text{th}}$ layer and the m^{th} neuron in the l^{th} layer and $b_m^{(l)}$ is the bias associated with the m^{th} neuron in the l^{th} layer.

Bayesian optimization and cross-validation are combined to determine the optimal hyperparameters Θ, including the number of layers, neurons, activation function type and learning rate. The optimization process starts by defining a search space for each hyperparameter. Then, cross-validation decomposes the training dataset into k folds, using a different fold each time as the validation set and the remaining k-1 for training. Until a convergence where the best performance is reached, the hyperparameters space is systematically explored by Bayesian optimization to identify those minimizing MSE through cross-validation:

$$\Theta^* = \arg\min_{\Theta} CV_{MSE}\left(MLP\left(\Theta; X_{train}^{std}, Y_{train}\right)\right) \qquad (6)$$

$CV_{MSE}\left(MLP\left(\Theta; X_{train}^{std}, Y_{train}\right)\right) = \frac{1}{k}\sum_{i=1}^{k} MSE\,(y_i, \hat{y}_i)$ is the average of the mean squared errors calculated across the different folds of cross-validation, X_{train}^{std} is the standardized training set and Y_{train} are the corresponding target values. The iterative process gradually refines the choice of hyperparameters, promoting the generalization beyond training data in an effective manner.

4 Experimental validation of DOA estimation

The training performance of the MLP model is validated by the learning curve depicted in Fig. 2b, which demonstrates the absence of overfitting and underfitting, as evidenced by the convergence of the training and cross-validation scores with the increasing size of the training set. Evaluation of the performance of the MLP model on the test set reveals high accuracy in estimating DOA with a mean square error (MSE) of $0.3°^2$. The results show that the MLP training model is robust against noisy data, an essential feature given the fixed objective that the model focuses on learning the trends in power distribution while disregarding noise and fluctuations between different samples. Fig. 2c presents the tight correlation between predicted and actual DOA values, where the linearity of the scattered points confirms the effectiveness of the model. Moreover, a detailed analysis of the prediction errors reveals that 94% of the predictions show less than 1° error, demonstrating the exceptional accuracy of the model.

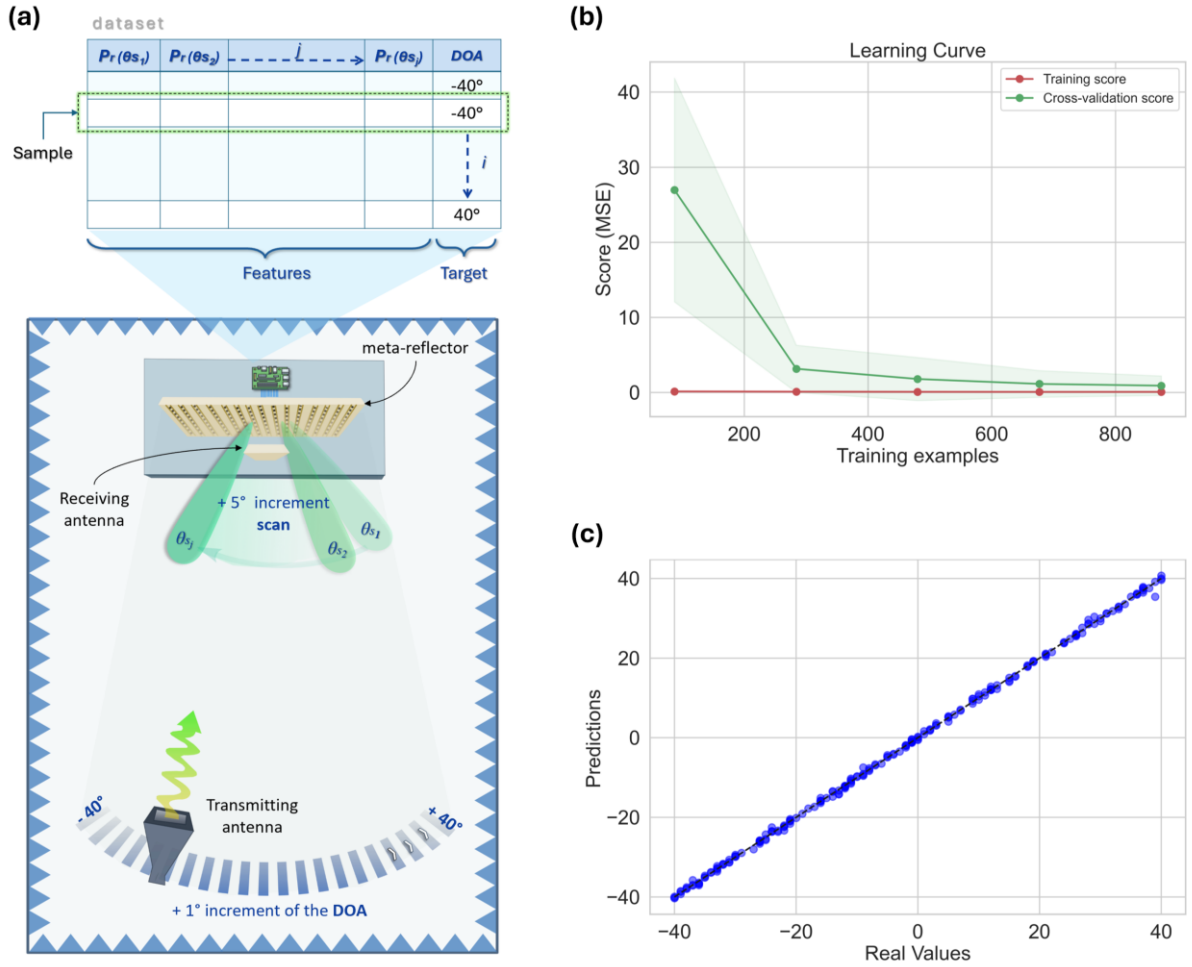

Figure 2: (a) Schematic principle of the metasurface-based platform for DOA estimation. (b) Learning curve of the MLP model for the DOA estimation. (c) Comparison of predicted vs. real DOA values.

5 Conclusions

In this work, a fast and accurate method for estimating DOA has been presented. The platform consists of a programmable metasurface reflector, assisted by deep learning. Our approach takes advantage of the flexibility and speed of reconfiguration of programmable metasurfaces to apply a series of parabolic phase profiles scanning the horizon in search of the direction of arrival of the incoming signal. As such, with a coarse angular scanning of the azimuth plane with step of 5°, the proposed system is able to estimate the DOA with an accuracy of 1°.

References

[1] S. Roger, M. Cobos, C. Botella-Mascarell, and G. Fodor, “Fast channel estimation in the transformed spatial domain for analog millimeter wave systems,” IEEE Trans. Wireless Commun., vol. 20, no. 9, pp. 5926–5941, 2021.

[2] G. Pau, F. Arena, Y. E. Gebremariam, and I. You, “Bluetooth 5.1: an analysis of direction finding capability for high-precision location services,” Sensors, vol. 21, no. 11, p. 3589, 2021.

[3] Y. Tian, S. Liu, W. Liu, H. Chen, and Z. Dong, “Vehicle positioning with deep-learning-based direction-of-arrival estimation of incoherently distributed sources,” IEEE Internet Things J., vol. 9, no. 20, pp. 20083–20095, 2022.

[4] M. Haardt, M. Pesavento, F. Roemer, and M. N. El Korso, “Subspace methods and exploitation of special array structures,” in Acad. Press Libr. Signal Process.: vol. 3 (Eds.: A. M. Zoubir, M. Viberg, R. Chellappa, S. Theodoridis), Elsevier, pp. 651-717, 2014.

[5] P. K. Eranti and B. D. Barkana, “An overview of direction-of-arrival estimation methods using adaptive directional time-frequency distributions,” Electronics, vol. 11, no. 9, p. 1321, 2022.

[6] V. Popov, B. Ratni, S. N. Burokur, and F. Boust, “Non-local reconfigurable sparse metasurface: efficient near-field and far-field wavefront manipulations,” Adv. Opt. Mater., vol. 9, no. 4, p. 2001316, 2021.

[7] R. Feng, B. Ratni, J. Yi, H. Zhang, A. de Lustrac, and S. N. Burokur, “Versatile metasurface platform for electromagnetic wave tailoring,” Photon. Res., vol. 9, no. 9, pp. 1650–1659, 2021.

[8] L. Li, H. Zhao, C. Liu, L. Long, and T. J. Cui, “Intelligent metasurfaces: control, communication and computing,” eLight, vol. 2, p. 7, 2022.

[9] B. Ratni, Z. Wang, K. Zhang, X. Ding, A. de Lustrac, G.-P. Piau, and S. N. Burokur, “Dynamically controlling spatial energy distribution with a holographic metamirror for adaptive focusing,” Phys. Rev. Appl., vol. 13, no. 3, p. 034006, 2020.

[10] T. V. Hoang, V. Fusco, M. A. B. Abbasi, and O. Yurduseven, “Single-pixel polarimetric direction of arrival estimation using programmable coding metasurface aperture,” Sci Rep, vol. 11, no. 1, Art. no. 1, 2021.

[11] J. W. Wang, Z. A. Huang, Q. Xiao, W. H. Li, B. Y. Li, X. Wan, and T. J. Cui, “High- precision direction- of- arrival estimations using digital programmable metasurface,” Adv. Intell. Syst., vol. 4, no. 4, p. 2100164, 2022.

[12] N. Meftah, B. Ratni, M. N. El Korso, and S. N. Burokur, “Programmable meta-reflector for multiple tasks in intelligent connected environments,” Adv. Mater. Technol., vol. 9, no. 12, p. 2400006, 2024.

[13] H.-Y. Li, H.-T. Zhao, M.-L. Wei, H.-X. Ruan, Y. Shuang, T. J. Cui, P. del Hougne, and L. Li, “Intelligent electromagnetic sensing with learnable data acquisition and processing,” Patterns, vol. 1, no. 1, p. 100006, 2020.

[14] C. Qian, B. Zheng, Y. Shen, L. Jing, L. Erping, L. Shen, and H. Chen, “Deep-learning-enabled self-adaptive microwave cloak without human intervention,” Nat. Photon., vol. 14, pp. 383–390, 2020.

[15] M. Huang, B. Zheng, T. Cai, X. Li, J. Liu, C. Qian, and H. Chen, “Machine-learning-enabled metasurface for direction of arrival estimation,” Nanophotonics, vol. 11, no. 9, pp. 2001-2010, 2022.

[16] B. Ratni, A. de Lustrac, G.-P. Piau, and S. N. Burokur, “Reconfigurable meta-mirror for wavefronts control: applications to microwave antennas,” Opt. Exp., vol. 26, no. 3, pp. 2613–2624, Feb. 2018.

[17] N. Meftah, B. Ratni, M. N. El Korso, and S. N. Burokur, “Enhanced-resolution learning-based direction of arrival estimation by programmable metasurface,” Adv. Electron. Mater., vol. 11, no. 3, p. 2400476, 2025.